HHS Public Access

Author manuscript

Environ Plan B Urban Anal City Sci. Author manuscript; available in PMC 2022 April 25.

Published in final edited form as:

Environ Plan B Urban Anal City Sci. 2022 March ; 49(3): 933–952. doi:10.1177/23998083211039854.

Modeling the Relationships Between Historical Redlining, Urban Heat, and Heat-Related Emergency Department Visits: An Examination of 11 Texas Cities

Dongying Li[1,*], **Galen D. Newman**[1], **Bev Wilson**[2,*], **Yue Zhang**[1], **Robert D. Brown**[1]

[1]Department of Landscape Architecture and Urban Planning, Texas A&M University, College Station, TX 77843, USA

[2]Urban and Environmental Planning, School of Architecture, University of Virginia, USA

Abstract

Place-based structural inequalities can have critical implications for the health of vulnerable populations. Historical urban policies, such as redlining, have contributed to current inequalities in exposure to intra-urban heat. However, it is unknown whether these spatial inequalities are associated with disparities in heat-related health outcomes. The aim of this study is to determine the relationships between historical redlining, intra-urban heat conditions, and heat-related emergency department visits using data from eleven Texas cities. At the zip code level, the proportion of historical redlining was determined, and heat exposure was measured using daytime and nighttime land surface temperature (LST). Heat-related inpatient and outpatient rates were calculated based on emergency department visit data that included ten categories of heat-related diseases between 2016 and 2019. Regression or spatial error/lag models revealed significant associations between higher proportions of redlined areas in the neighborhood and higher LST (Coef. = 0.0122, 95% CI = 0.0039 - 0.0205). After adjusting for indicators of social vulnerability, neighborhoods with higher proportions of redlining showed significantly elevated heat-related outpatient visit rate (Coef. = 0.0036, 95% CI = 0.0007-0.0066) and inpatient admission rate (Coef. = 0.0018, 95% CI = 0.0001-0.0035). These results highlight the role of historical discriminatory policies on the disparities of heat-related illness and suggest a need for equity-based urban heat planning and management strategies.

Keywords

Redlining; urban heat; heat-related illness; climate change; environmental justice

1. Introduction

Place-based socio-ecological inequities can have critical impacts on health outcomes (Krieger, 2014). It is well-documented that disadvantaged neighborhoods experience higher burdens of health risks (Diez Roux and Mair, 2010; Ross and Mirowsky, 2001). Research

[*]Corresponding Author: Dongying Li, Address: Department of Landscape Architecture and Urban Planning, Texas A&M University, Langford A 337, TAMU 3137, College Station, TX, 77845. dli@arch.tamu.edu.

from the past two decades has further clarified the distinction between compositional effects (i.e., population composition) and contextual effects (i.e., the neighborhood environment) that impact health outcomes (Kawachi and Berkman, 2003). Housing characteristics and infrastructure-related factors rooted in the spatial patterns of public and private investment/disinvestment influence health outcomes, independent of the sociodemographic characteristics of the population. Recently, an emerging body of research has called for in-depth investigation into place-based health disparities stemming from historical and/or structural segregation and racism (Schell et al., 2020; Butler et al., 2020). Redlining was one such policy that formalized racial and ethnic discrimination in mortgage lending and further entrenched residential segregation (Rothstein, 2017). In this study, historical redlining refers to the New Deal-era discriminatory policy of disinvestment in communities with higher minority populations (Zenou and Boccard, 2000).

Extreme heat already exerts a serious toll on communities, with a mortality rate twice that of storms and floods (Thacker et al., 2008). Global climate change makes the need to identify heat risks and mitigate their public health effects more urgent As the frequency, intensity, and duration of hot days and extreme heat events continues to increase, rising heat-related mortality and morbidity rates are likely to become severe societal challenges (Petkova et al., 2013; Guo et al., 2018). Previous studies have revealed racial and socioeconomic disparities with respect to heat-related mortality and morbidity (Chan et al., 2012; Anderson and Bell, 2009; Rosenthal et al., 2014; Gronlund, 2014). These socioeconomic and demographic factors that affect susceptibility of different groups to environmental hazards, often described as social vulnerability (Cutter et al., 2003), may help to explain observed disparities in heat-related mortality and morbidity.

Most recently, significant advances have been made in understanding whether neighborhoods historically targeted for discriminatory mortgage policies are associated with disproportionate sorting of infrastructure and environmental stressors such as intra-urban heat exposure. For example, a study using satellite imagery from between 2014 and 2017 for 108 urban areas in the U.S. demonstrated that historically redlined areas experience higher land surface temperature compared to non-redlined areas (Hoffman et al., 2020). This pattern was confirmed in another study that focused on Baltimore, Dallas, and Kansas City and used land surface temperatures derived from imagery obtained between 2018 and 2020 (Wilson, 2020). However, as heat-related illness is attributable not only to ambient heat conditions, but also to environmental and social protective/coping resources, along with individual pre-existing health conditions, it is unknown whether these differences in surface temperature result in differences in the rate of heat-related illnesses. Therefore, the extent to which historically redlined neighborhoods show elevated heat exposure and report higher rates of heat-related illnesses must be assessed and such an investigation will provide evidence for heat-related health interventions and inform policies designed to remedy disparities in heat exposure attributable to structural segregation.

This article addresses the following research questions: (1) do urban areas where a higher proportion of the land area was formerly redlined experience higher diurnal land surface temperatures and heat-related emergency department admissions relative to other areas; and (2) do the associations between the proportion of redlined land area and heat-related

emergency department visits persist after controlling for social vulnerability? We use data from eleven Texas cities to extend the emerging evidence related to inequalities in heat exposure to heat-related health risks. The high heat-related risks of these Texas cities stems from both their geographic location spanning three relatively hot climate subtypes, and their tremendous urban growth, which averaged 20.8% between 2000 and 2019. Land use and the built environment contribute directly to heat exposure in cities through the urban heat island (UHI) effect, which is intensified by factors like impervious surfaces and albedo materials (Stone Jr and Rodgers, 2001). These factors are compounded by historical planning practices of prioritizing urban growth, industry, highways, and impervious surfaces. Further, the Gulf Coast region is home to a disproportionately large number of communities and people who are socially vulnerable to environmental hazards and the region is often considered a critical area for advancing environmental equity. The primary objective of this study is to examine the relationships between diurnal land surface temperatures, heat-related health facility visit rates, and historical redlining, while adjusting for neighborhood-level social vulnerability.

1.1 Historical Redlining and Environmental Inequalities

Policies contributing to residential segregation were widespread in the decade following the Great Depression. Redlining was a particularly widespread and consequential policy enabled by the Home Owners' Loan Corporation (HOLC) that mapped "mortgage security" grades in more than 200 cities in the United States. The HOLC was formed to control mortgage risks, address underwater mortgages, and foreclosed properties (An et al., 2019; Hillier, 2003). In assessing foreclosure risk, the HOLC assigned four grades to residential areas in cities: A-best, B-still desirable, C-definitely declining, and D-hazardous. These grades were based on entire neighborhoods, rather than individual properties, according to a "City Survey Program" that rated the ethnicity, income, and occupation of residents along with housing conditions, explicitly discriminating against African Americans, Hispanics, and other minorities (Jackson, 1980; Jackson, 1987; An et al., 2019; Hillier, 2003). As a government body, the HOLC institutionalized residential segregation and directed certain investments and disinvestments in targeted communities. Although the HOLC was abolished in less than 15 years, its results continued to influence patterns of economic and social inequality (Mitchell and Franco, 2016). Over time, these structured segregations and systematic disadvantages were further exacerbated, leading to severe socio-environmental disparities.

Redlining, as a racist government policy that continues to impact communities of color, has far-reaching implications beyond the observed socio-economic conditions alone. These implications include how public investments were distributed and how public institutions regulated and incentivized private sector investments. As a result, housing segregation, infrastructure degradation, concentrations of environmental hazards, segregated schools, and denial of equal access to opportunities for the next generation all contribute to the complex landscape of place-based inequalities. Studies have revealed that legacies of redlining are associated with poverty, income inequality, education deprivation, infrastructure and built environment deterioration, and diminished home value (Sadler and Lafreniere, 2017; Curtis and O'Connell, 2017; Rothstein, 2017; Mitchell and Franco, 2016). Related to

infrastructure, prior studies have found significantly lower densities of vegetation cover in redlined areas (Wilson, 2020; Nardone et al., 2021). In addition, highways and toxic-hazard sites were often constructed in marginalized areas (Nardone et al., 2020a), as these residents often have fewer resources to resist the siting of a potentially hazardous facility.

Recent studies have situated the discussion of residential segregation within the larger environmental justice and environmental health conversation. The structural inequalities created and perpetuated by redlining contribute to persistent patterns of urban infrastructural and landscape heterogeneity, governing the distributions of land cover, contaminants, green space and its ecosystem services, as well as disease dynamics (Schell et al., 2020; Sailor et al., 2019). For example, urban tree canopy, which plays a vital role in mitigating heat exposure, has been shown to be consistently lower in African-American, Hispanic, and lower-income neighborhoods (Kolosna and Spurlock, 2019). However, recent research has also linked redlining to air quality and disparities in exposure to airborne hazards (e.g., particulate matter) that are mediated by factors like tree canopy and the filtering benefits thereof (Namin et al., 2020). As such, the examination of historical unequal housing policies along with current incidences and distributions of health risks will offer insights into the shaping of place-based inequalities.

1.2 Historical Redlining, Health Disparities, and Heat Exposure

Current and historical residential segregation and lending biases have been linked to numerous health risks and outcomes. For example, present-day lending biases (e.g., likelihood of racial minorities being denied mortgages) have been associated with breast cancer mortality (Collin et al., 2020; Beyer et al., 2016). Most recently, an emerging body of literature has revealed associations between historical redlining and present-day morbidity and mortality in urban areas. For example, residing in historically redlined neighborhoods is associated with higher odds of preterm birth and worse birth outcomes (Krieger et al., 2020a; Nardone et al., 2020b). Populations in historically redlined areas also show elevated risks of lung cancer and breast cancer, even in neighborhoods with high present-day socioeconomic privileges (Krieger et al., 2020b). Likewise, emergency department visits due to asthma were found to be elevated in historically redlined areas in California (Nardone et al., 2020a).

One particular health outcome that is increasingly tied to the spatial characteristics of cities is urban heat stress and heat-related health. Studies have demonstrated correlations of sociodemographic and housing conditions with heat vulnerability (Gronlund, 2014; Johnson et al., 2012). The health burden caused by heat stress falls disproportionately on groups that are physiologically sensitive to heat events or have less adaptive resources, such as the elderly, the poor, and the socially isolated (Klinenberg, 2015). Worse still, historically redlined neighborhoods not only have higher percentages of socioeconomically disadvantaged residents, but also more degraded housing and infrastructure which perform poorly during heat events, have less heat mitigation amenities, and experience higher levels of ambient heat exposure (Harlan et al., 2006).

Recent studies revealed critical linkages between historical residential segregation and intra-urban land surface temperature (LST). A study investigating LST patterns in 108 US urban

areas found that in 94% of those areas, redlined and non-redlined neighborhoods displayed significantly different LSTs (Hoffman et al., 2020). The gap in average LST was 2.6 °C across all 108 cities, and up to 7 °C within a city (Hoffman et al., 2020). Another study focusing on Baltimore, Dallas, and Kansas City confirmed historically redlined neighborhoods to experience higher LST, and suggested a need for environmental justice discussions related to urban planning based on this finding (Wilson, 2020).

As heat exposure is a strong risk factor for heat-related illness, a critical question to ask is whether neighborhoods with a larger proportion of historically redlined areas experience worse heat-related health outcomes relative to less-redlined neighborhoods. If the differences in neighborhood-level land surface temperature are of a magnitude that causes disparities in heat-related health conditions, then these thermal inequalities in the built environment require immediate attention of planners, policymakers, and public health providers. In that case, collaborative environmental and public health efforts to mitigate the impacts of historical residential segregation on place-based heat vulnerabilities may be warranted.

2. Methods

2.1 Study Area

Eleven cities from Texas were included in this study, selected on the diversity of climate conditions and availability of historical redlining data. These cities are Amarillo, Austin, Beaumont, Dallas, El Paso, Fort Worth, Galveston, Houston, Port Author, San Antonio, and Waco. This list includes the top six populated cities in Texas, and three different Köppen-Geiger climate subtypes (Köppen, 1900; Köppen and Geiger, 1930). The Köppen-Geiger climate classification identifies climatically similar zones based on factors such as temperature and rainfall. Selecting study sites in multiple geographic and climatic zones typically increases the generalizability of the findings. In addition, many of these Texas cities have demonstrated unprecedented urbanization and rapid urban heat island intensification over the past few decades (Streutker, 2003; Hu and Xue, 2016).

2.2 Constructs and Measures

2.2.1 Historical Redlining—Historical redlining was defined based on the historical HOLC grades assigned to residential areas: A-best, B-still desirable, C-definitely declining, and D-hazardous (Figure 1). Redlining maps were obtained from the geo-rectified data from the Mapping Inequality project of the University of Richmond (Hernandez, 2009). The unit of analysis for this study was zip code tabulation area (ZCTA), created by the U.S. Census Bureau to represent the areal boundaries of the United States Postal Services zip codes. As the spatial boundaries of redlined zones do not match the ZCTAs, we calculated the areal proportions of each ZCTA that fall within each of the four HOLC classes. In particular, we examined the proportion assigned grade C (definitely declining) or grade D (hazardous) as redlined. To perform direct comparisons between ZCTAs that encompass higher proportions of redlined (C- and D-graded) zones and those that intersect with few redlined zones, we categorized the proportion of redlined zones variable based on 50%

percentile; the yielded two-categories are referred to in the present study as *more-redlined* and *less-redlined* ZCTAs.

2.2.2 Land Surface Temperature—Land surface temperature (LST) is a widely used measure for capturing heat hazards and comparing urban heat exposure across different areas. Although LST does not fully capture the set of micrometeorological conditions that factor into human thermal comfort or heat stress, recent studies have shown strong correlations between LST and air temperature (Good et al., 2017), and validated the use of LST to infer thermal comfort, such as the Physiological Equivalent Temperature (PET) (Goldblatt et al., 2021). Compared to other measures such as air and surface temperature values taken at meteorological stations with coarse spatial resolution, satellite imagery derived LST presents data at higher spatial resolutions, thereby enabling comparisons among different neighborhoods. Recent studies assessing heat-related vulnerability and population health risks have relied on LST as the most widely used meteorological indicator (Inostroza et al., 2016; Buscail et al., 2012; Weber et al., 2015; Loughnan et al., 2012). In this study, we used surface temperature data retrieved from the ECOSTRESS Land Surface Temperature and Emissivity products recently released by the National Aeronautics and Space Administration (NASA) (Hook and Hulley, 2019). This dataset offers fine-scaled atmospherically-corrected imagery throughout diurnal cycles at a 70m spatial resolution base on MODIS data, which allows the estimation of daytime and nighttime LSTs. Recent studies have utilized ECOSTRESS data to evaluate heat vulnerability and reveal fine-scale heat exposure information (Hulley et al., 2019).

Specifically, LST data from the ECO2LSTE product within the June 1st and August 31st, 2018-2020 window that covered the selected urban areas were downloaded. Also obtained were the quality control data and cloud cover ECO2CLD products. The imagery was screened to ensure minimum cloud coverage, and best/normal quality pixels were flagged based on retrieval and atmospheric conditions. One daytime and one nighttime imagery set with best quality flags were selected for each city (Figure 2), and summary measures such as mean daytime/nighttime LST, minimum daytime/nighttime LST, and maximum daytime/nighttime LST were determined with reference to ZCTA boundaries.

2.2.3 Social Vulnerability Factors—Social vulnerability is defined as the demographic and socioeconomic factors that affect the susceptibility of the population to heat-related health risks. Heat-related health literature has demonstrated that, in addition to heat hazard (as measured by ambient/surface temperature), social vulnerability factors explain the sensitivity of a population to heat stress as well as its adaptability and resources for mitigating the negative health impacts. Based on a review of heat vulnerability models/indices, we identified the most common social vulnerability indicators (Nayak et al., 2018; Reid et al., 2009) included in determining population heat vulnerability: population aged 65 and older, non-White population, Hispanic population, lower-income population, individuals living alone, and populations who do not speak English well. These variables were derived from the American Community Survey 2015-2019 five-year estimates at the ZCTA scale and normalized by the total population.

2.2.4 Heat-Related Emergency Department Visits—

Heat-related emergency department (ED) visits were extracted from data provided by the Texas Center for Health Statistics, Department of State Health Services. This dataset included all inpatient and outpatient ED records between 2016 and 2019 for approximately 495 hospitals/facilities (with ~5 yearly variations) across the entire state. For example, in 2016, there was a total of 10,486,677 ED visits, of which 1,471,871 (13.8%) were admitted and recorded in the inpatient category while the rest were in the outpatient category. Each record included one primary diagnosis and up to 24 additional diagnoses, coded based on the International Classification of Diseases, 10th revision (ICD-10). Other available information for each record included the patient's sex, age, race, and ethnicity, as well as data related to billing and charges. Due to confidentiality and privacy constraints, geographic information was only released at the zip code level and the specific date of an ED visit was also not available.

We considered an ED visit to be heat-related if the patient was assigned at least one of the following diagnoses: heatstroke and sunstroke (T67.0); heat syncope (T67.1); heat cramp (T67.2); heat exhaustion, anhidrotic (T67.3); heat exhaustion due to salt depletion (T67.4); heat exhaustion, unspecified (T67.5); heat fatigue, transient (T67.6); heat edema (T67.7); other effects of heat and light (T67.8); effect of heat and light, unspecified (T67.9); and exposure to excessive natural heat (X30). These ICD-10 classes have been used in studies examining heat vulnerability and heat-related diseases as caused by heat waves and environmental conditions (Schaffer et al., 2012; Gronlund et al., 2015). ZCTA-level rates of heat-related ED visits were then calculated as inpatient and outpatient counts weighted by the total population.

2.3 Statistical Analysis

All data preparation and statistical analyses were performed using R packages. Independent-sample *t*-tests and boxplots were generated to demonstrate the extent to which the LST and heat-related ED visit rates differed by more-redlined and less-redlined ZCTAs.

To determine whether these relationships hold after adjusting for social vulnerability controls and spatial dependency, we tested ordinary least squares (OLS) models and spatial models on LST and heat-related ED visits. The distributions of outcome variable distributions were examined and the values transformed as needed; specifically, square root transformation was used for both inpatient and outpatient rates. We examined spatial autocorrelation in the residuals. When Moran's I was non-significant, we decided spatial autocorrelation was absent and proceeded with the OLS. When Moran's I was significant, we decided that the OLS would yield biased estimates, and therefore used a spatial autoregressive model (SAR) instead. In SAR, spatial dependence is addressed either as a spatially lagged dependent variable (spatial lag model) or in the error structure (spatial error model) (Anselin and Bera, 1998; Cressie, 2015). The formulas of the two models are given below. The Lagrange Multiplier (LM) test was used to determine the appropriate model. Breusch-Pagan tests for heteroscedasticity were used, and upon revealing significant heteroscedasticity, corrections (1980) were applied.

$$y = \rho Wy + X\beta + \varepsilon \quad \text{(Equation 1)}$$

where Wy is the lagged dependent variable, ρ is the spatial autoregressive coefficient, and ε is the error term.

$$y = X\beta + \mu; \mu = \lambda W\mu + \varepsilon \quad \text{(Equation 2)}$$

where μ is the vector that represents the spatially autocorrelated error term, λ is the spatial autoregressive coefficient, Wμ is the spatial lag for the errors, and ε is the error term.

3. Results

3.1 Characteristics of Study Areas and Population

Table 1 presents ZCTA-level descriptive statistics and comparisons between areas with high and low proportions of redlined areas. The average population per ZCTA was about 24,000, with 18% of the population being aged 65 or older. Overall, the study areas showed high racial and ethnic diversity: the mean proportion of the non-White population was 30% and the mean proportion of the Hispanic population was 45%. Demographically, more-redlined ZCTAs did not differ significantly regarding total population, housing units, or age composition relative to less-redlined ZCTAs. However, they had about 50% higher percentage of Hispanic population compared to less-redlined ZCTAs. Further, socioeconomic gaps were statistically significant between high- and less-redlined areas: more-redlined ZCTAs showed a 40% higher low-income population, 20% more people living alone, and 85% more individuals who did not speak English well.

Across all ZCTAs, the mean daytime LST was 36.17 °C and the nighttime LST was 28.55 °C. Figure 3 shows boxplots that better represent the comparative distributions of heat exposure and heat-related ED visits. Overall daytime LST data varied with greater magnitude than nighttime LST, as daytime surfaces are heated directly by solar radiation, areas with less tree canopy will likely have higher temperatures; meanwhile, at night, areas with less canopy cover will emit more terrestrial radiation to the sky, thus achieving nighttime temperatures similar to areas with more canopy. More-redlined ZCTAs demonstrated a 3.90 °C hotter daytime surface temperature and a 0.87 °C nighttime surface temperature than less-redlined ones, including higher mean daytime LST, daytime min LST, mean nighttime LST, and nighttime max LST (Table 1). Figure 3 confirms these results and reveals that the values for the lower quartile, median, and upper quartile for daytime LST, nighttime LST are all higher for more-redlined areas.

For emergency department visits, there were a total of 5,229 inpatient and 39,241 outpatient records that had at least one heat-related diagnosis. Both inpatient and outpatient rates were significantly different between high- and less-redlined areas. The population-weighted inpatient admission rate of more-redlined areas was about 87% percent above that of less-redlined areas, and the outpatient rate was likewise about 50% greater. Detailed information at the patient-level is presented in Supplementary Material Table S1.

3.2 Heat Exposure and Historical Redlining

To examine whether heat exposure varied by historical redlining, we fitted OLS models predicting daytime and nighttime LST based on proportion of redlining and examined the residual spatial autocorrelation. For both daytime and nighttime models, the Moran's I statistic was significant ($p < 0.0001$) and LMerr and LMag robust tests favored the spatial lag model (RLMlag < 0.001). Therefore, the spatial lag model (Equation 1) was selected for further modeling.

The results from the spatial lag models (Table 2) showed that the proportion of redlining was a significant predictor of daytime LST (Coef. = 0.0122, 95% CI = 0.0039 - 0.0205). Similarly, a greater proportion of redlining was associated with higher nighttime LST (Coef. = 0.0098, 95% CI = 0.005 - 0.0146).

3.3 Heat-Related Emergency Department Visits and Historical Redlining

We likewise determined appropriate models for heat-related emergency department visit rates by examining the spatial autocorrelation of OLS model residuals. For Models 3 and 4, we predicted inpatient admission rates first using only social vulnerability data; and then added in the redlining factor. For both models, Moran's I failed to detect residual spatial autocorrelation ($p > 0.05$), thus the OLS models were presented. For Models 5 and 6, we predicted outpatient visit rates using social vulnerability factors alone; and then social vulnerability factors plus redlining. With these models, the Moran's I statistic showed significant spatial autocorrelation ($p < 0.001$) and the LMerr tests favored spatial error models ($p < 0.001$), thus the spatial error models (Equation 2) were selected for fitting outpatient data.

Model 3 showed that of all social vulnerability variables, percent older population (Coef. = 0.0076, 95% CI = 0.0034-0.0118), lower-income population (Coef. = 0.0089, 95% CI = 0.0038-0.0139), and individuals living alone (Coef. = 0.0055, 95% CI = 0.0016-0.0095) were significantly related to higher inpatient admission rates (Table 3). Race, ethnicity, and language spoken were not significantly correlated. After adding in redlining, Model 4 revealed a significant association of redlining with inpatient admission rates (Coef. = 0.0018, 95% CI = 0.0001-0.0035); the higher the proportion of areas historically categorized as "definitely declining" or "hazardous," the higher the present-day heat-related inpatient rates. Older age, low income, and social isolation remained significant social vulnerability factors.

When spatial error models were tested for outpatient visit rates, the results were mostly consistent with inpatient rates (Table 4). In both Models 5 and 6, older, low-income, and socially isolated populations had significant associations with heat-related outpatient visit rates. A higher proportion of redlined areas was also significantly associated with heat-related outpatient visits (Coef. = 0.0036, 95% CI = 0.0007-0.0066). Similarly, race, ethnicity, and language factors were not statistically significantly associated with ED visit rates.

4. Discussion

4.1 Interpretation of Results

Our results showed that daytime and nighttime mean LST were significantly higher in ZCTAs with higher proportions of redlined areas, which is consistent with previous studies using different units of analysis (Hoffman et al., 2020; Wilson, 2020). Taken together, these results suggest that inequalities in urban heat island conditions exist not only between the historically defined redlined and non-redlined zones, but also between contemporary geographic units that contain more versus fewer historically redlined areas.

Possible mechanisms explaining the hotter surface temperature in areas with more-redlined neighborhoods include a variety of built environmental factors such as less vegetation, more impervious surfaces, more transportation infrastructure, and distinct housing typology. The literature has confirmed that vegetation cover is often denser in more affluent, predominantly White neighborhoods, while impervious surfaces are more prevalent in racial and ethnic minority neighborhoods (Hoffman et al., 2020; Nowak and Greenfield, 2018). Specifically, one study showed that A-graded areas now have almost twice as much tree canopy cover relative to D-graded redlined areas (Locke et al., 2020). More highway and parking lot constructions and high-density multifamily housing typology are also characteristics of areas historically discriminated against (An et al., 2019; Bös, 2015; Hirsch, 2009); these urban typology factors have been shown to influence the urban thermal environment (Yin et al., 2018).

Beyond ambient surface temperature, our results also uncovered associations between the legacy of redlining and present-day thermal health outcomes. Areas with higher proportions of historically redlined zones experience higher population-adjusted emergency department visits with heat-related diagnoses, even after adjusting for social vulnerabilities. To our knowledge, these are the first results linking heat-related emergency department data to historical discriminatory housing policies. These results suggest that contextual factors are related to higher heat risks (Kawachi and Berkman, 2003), and these effects persist after accounting for compositional factors (i.e., the demographic and socioeconomic conditions of the population).

Although our study is observational, higher daytime and nighttime land surface temperatures could be the reason for elevated incidences of heat-related illness, a finding supported by studies evaluating heat-related health risks using LST as the main heat exposure indicator (Buscail et al., 2012; Ho et al., 2015). Other possible mechanisms may include built environment and infrastructure factors such as poor housing conditions (Samuelson et al., 2020), low A/C availability (Santamouris et al., 2020), lack of cooling centers (Fraser et al., 2018), and shaded recreational areas (Johnson et al., 2012; Nayak et al., 2018); all of which have been identified as environmental factors contributing to high levels of heat-related morbidity and mortality. These results, in accordance with recent studies on population risks related to cancer (Krieger et al., 2020b), asthma (Nardone et al., 2020a), and birth outcomes (Krieger et al., 2020a; Nardone et al., 2020b), as well as on self-reported health (McClure et al., 2019), outline critical health disparities rooted in historical residential segregation, and call for policy intervention to aid populations experiencing such place-based inequalities.

Climate change poses severe challenges to community health. Our findings suggest that these challenges are distributed unevenly, and that historically redlined neighborhoods bear a disproportionately heavy burden. Existing heat-hazard prevention and mitigation plans are mostly based on entire region or city-level conditions while few policies and initiatives pay attention to the inequalities rooted in long-standing spatial patterns of disinvestment and segregation in cities. Understanding how disparities in heat-related health conditions may have emerged through historical housing segregation can focus attention and resources on redressing these inequalities. Furthermore, the recognition that land surface temperature and social vulnerabilities each explain part of the variance in heat-related emergency department visit rates suggests the importance of addressing infrastructure degradation in redlined areas from a public health perspective. It also calls attention to social programs to promote the adaptive capacity and coping resources for socioeconomically disadvantaged neighborhoods and individuals underscoring the need for mitigation efforts that bring socio-ecological solutions to bear on the multiple challenges arising from structural inequalities.

4.2 Limitations and Future Directions

Several limitations of this study need to be noted. Firstly, heat-related emergency department visit counts cannot fully represent rates of heat-related illness. For example, the most financially disadvantaged populations may not visit a hospital or clinic's emergency department. Although the racial compositions of the ED visit data generally were similar to Census data, the percentage of Hispanic residents in ED visits was lower than in the overall population. Therefore, it is possible that, even with significant relationships detected in the present results, the extent of heat-related health disparities between redlined and non-redlined areas may still be underestimated. Secondly, the LST data used as proxy for heat exposure may not fully capture the complete energy input and output that determine human thermal experience. Although previous studies have established strong links between LST and thermal comfort and heat health risks (Goldblatt et al., 2021), during heat events, incident solar radiation can be the most critical element influencing the energy budget exchange between human body and the environment (Brown and Gillespie, 1995). Therefore, advances in measuring and modeling micrometeorological conditions may offer new insights into the fine-grained spatial disparities in heat exposure. Thirdly, due to privacy restrictions regarding the data provided by the Texas Center for Health Statistics, ED data were spatially aggregated to the Zip Code Tabulation Area (ZCTA) level, and neither individual sociodemographic characteristics nor the date of emergency department visits was available. As such, we were unable to conduct individual-level analysis or filter the dataset to include only records following heat waves. In addition, our results pertain more to the overall patterns of heat-related illness, which could be different than the patterns during specific heat waves or extremely hot days. Future studies should seek to use individual-level medical records or emergency department data and test case-crossover models or survival models to investigate the historical legacy of redlining and disinvestment on heat-related illness during heat waves and extreme weather conditions. Moreover, although this study considered social vulnerability indicators such as demographics, socioeconomics, and social isolation, environmental and housing related factors such as ventilation, and A/C availability, and neighborhood topography, tree canopy cover, impervious surface, and water bodies were not considered. These factors are likely to be mediators between historical redlining and

health outcomes; therefore, more comprehensive heat risk assessments need be made that take into consideration all factors related to heat exposure, sensitivity, and adaptability.

In addition, our study revealed heat-related health disparities based on the patterns of historical redlining. It is worth noting that, since there were pre-existing sociodemographic and environmental differences between redlined and non-redlined neighborhoods at the time of the policy, the argument that redlining itself is the direct cause of heat-related health disparities needs to be made with caution. Historical redlining, as an official policy institutionalizing residential segregation and discrimination, may very well influence social and environmental dynamics through complex pathways and interrelationships. Longitudinal studies that can account for historical changes in the social, environmental, and heat conditions of redlined neighborhoods may uncover the complex processes that link contextual and compositional disadvantages.

4.3 Conclusion

This article contributes to a growing literature that explores the connection between discriminatory urban development policies and heat-related health disparities. This research corroborates prior research about elevated land surface temperatures in historically redlined areas and extends the discussion to heat-related illness. To our knowledge, this study is the first of its kind to uncover the relationships between historical redlining, elevated land surface temperatures, and heat-related healthcare facility admissions. Our findings suggest that the uneven distribution of health risks to heat are linked to both neighborhood environmental and sociodemographic factors and must be explicitly recognized as such in order for truly equitable heat resilience planning to occur.

Supplementary Material

Refer to Web version on PubMed Central for supplementary material.

References

An B, Orlando AW and Rodnyansky S (2019) The physical legacy of racism: How redlining cemented the modern built environment. Available at SSRN 3500612.

Anderson BG and Bell ML (2009) Weather-related mortality: how heat, cold, and heat waves affect mortality in the United States. Epidemiology (Cambridge, Mass.) 20(2): 205.

Anselin L and Bera AK (1998) Introduction to spatial econometrics. Handbook of applied economic statistics 237.

Beyer KM, Zhou Y, Matthews K, et al. (2016) New spatially continuous indices of redlining and racial bias in mortgage lending: links to survival after breast cancer diagnosis and implications for health disparities research. Health & place 40: 34–43. [PubMed: 27173381]

Bös M (2015) Rasse und Ethnizität: zur Problemgeschichte zweier Begriffe in der amerikanischen Soziologie. Springer-Verlag.

Brown RD and Gillespie TJ (1995) Microclimatic landscape design: creating thermal comfort and energy efficiency. Wiley New York.

Buscail C, Upegui E and Viel JF (2012) Mapping heatwave health risk at the community level for public health action. International Journal of Health Geographics 11.

Butler B, Outrich M, Roach J, et al. (2020) Generational Impacts of 1930s Housing Discrimination and the Imperative Need for the Healthy Start Initiative to Address Structural Racism. Journal of Health Disparities Research and Practice 13(3): 4.

Chan EYY, Goggins WB, Kim JJ, et al. (2012) A study of intracity variation of temperature-related mortality and socioeconomic status among the Chinese population in Hong Kong. J Epidemiol Community Health 66(4): 322–327. [PubMed: 20974839]

Collin LJ, Gaglioti AH, Beyer KM, et al. (2020) Neighborhood-level redlining and lending bias are associated with breast cancer mortality in a large and diverse metropolitan area. Cancer Epidemiology and Prevention Biomarkers.

Cressie N (2015) Statistics for spatial data. John Wiley & Sons.

Curtis KJ and O'Connell HA (2017) Historical racial contexts and contemporary spatial differences in racial inequality. Spatial demography 5(2): 73–97. [PubMed: 29736409]

Cutter SL, Boruff BJ and Shirley WL (2003) Social vulnerability to environmental hazards. Social science quarterly 84(2): 242–261.

Diez Roux AV and Mair C (2010) Neighborhoods and health.

Goldblatt R, Addas A, Crull D, et al. (2021) Remotely Sensed Derived Land Surface Temperature (LST) as a Proxy for Air Temperature and Thermal Comfort at a Small Geographical Scale. Land 10(4): 410.

Good EJ, Ghent DJ, Bulgin CE, et al. (2017) A spatiotemporal analysis of the relationship between near-surface air temperature and satellite land surface temperatures using 17 years of data from the ATSR series. Journal of Geophysical Research: Atmospheres 122(17): 9185–9210.

Gronlund CJ (2014) Racial and socioeconomic disparities in heat-related health effects and their mechanisms: a review. Current epidemiology reports 1(3): 165–173. [PubMed: 25512891]

Gronlund CJ, Berrocal VJ, White-Newsome JL, et al. (2015) Vulnerability to extreme heat by sociodemographic characteristics and area green space among the elderly in Michigan, 1990–2007. Environmental research 136: 449–461. [PubMed: 25460667]

Guo Y, Gasparrini A, Li S, et al. (2018) Quantifying excess deaths related to heatwaves under climate change scenarios: A multicountry time series modelling study. PLoS medicine 15(7).

Harlan SL, Brazel AJ, Prashad L, et al. (2006) Neighborhood microclimates and vulnerability to heat stress. Social Science & Medicine 63(11): 2847–2863. [PubMed: 16996668]

Hernandez J (2009) Redlining revisited: mortgage lending patterns in Sacramento 1930–2004. International Journal of Urban and Regional Research 33(2): 291–313.

Hillier AE (2003) Redlining and the home owners' loan corporation. Journal of Urban History 29(4): 394–420.

Hirsch AR (2009) Making the second ghetto: Race and housing in Chicago 1940-1960. University of Chicago Press.

Ho HC, Knudby A and Huang W (2015) A Spatial Framework to Map Heat Health Risks at Multiple Scales. International Journal of Environmental Research and Public Health 12(12): 16110. [PubMed: 26694445]

Hoffman JS, Shandas V and Pendleton N (2020) The effects of historical housing policies on resident exposure to intra-urban heat: A study of 108 US urban areas. Climate 8(1): 12.

Hook S and Hulley G (2019) ECOSTRESS Land Surface Temperature and Emissivity Daily L2 Global 70 m V001 [Data set]. NASA EOSDIS Land Processes DAAC.

Hu X-M and Xue M (2016) Influence of synoptic sea-breeze fronts on the urban heat island intensity in Dallas–Fort Worth, Texas. Monthly Weather Review 144(4): 1487–1507.

Hulley G, Shivers S, Wetherley E, et al. (2019) New ECOSTRESS and MODIS land surface temperature data reveal fine-scale heat vulnerability in cities: A case study for Los Angeles County, California. Remote Sensing 11(18): 2136.

Inostroza L, Palme M and de la Barrera F (2016) A Heat Vulnerability Index: Spatial Patterns of Exposure, Sensitivity and Adaptive Capacity for Santiago de Chile. PLoS ONE 11(9).

Jackson KT (1980) Race, ethnicity, and real estate appraisal: The home owners loan corporation and the federal housing administration. Journal of Urban History 6(4): 419–452.

Jackson KT (1987) Crabgrass frontier: The suburbanization of the United States. Oxford University Press.

Johnson DP, Stanforth A, Lulla V, et al. (2012) Developing an applied extreme heat vulnerability index utilizing socioeconomic and environmental data. Applied Geography 35(1-2): 23–31.

Kawachi I and Berkman LF (2003) Neighborhoods and health. Oxford University Press.

Klinenberg E (2015) Heat wave: A social autopsy of disaster in Chicago. University of Chicago Press.

Kolosna C and Spurlock D (2019) Uniting geospatial assessment of neighborhood urban tree canopy with plan and ordinance evaluation for environmental justice. Urban forestry & urban greening 40: 215–223.

Köppen W (1900) Versuch einer Klassifikation der Klimate, vorzugsweise nach ihren Beziehungen zur Pflanzenwelt. Geographische Zeitschrift 6(11. H): 593–611.

Köppen W and Geiger R (1930) Handbuch der klimatologie. Gebrüder Borntraeger Berlin.

Krieger N (2014) Discrimination and health inequities. International Journal of Health Services 44(4): 643–710. [PubMed: 25626224]

Krieger N, Van Wye G, Huynh M, et al. (2020a) Structural Racism, Historical Redlining, and Risk of Preterm Birth in New York City, 2013–2017. American Journal of Public Health.(0): e1–e8.

Krieger N, Wright E, Chen JT, et al. (2020b) Cancer Stage at Diagnosis, Historical Redlining, and Current Neighborhood Characteristics: Breast, Cervical, Lung, and Colorectal Cancer, Massachusetts, 2001-2015. American Journal of Epidemiology.

Locke D, Hall B, Grove JM, et al. (2020) Residential housing segregation and urban tree canopy in 37 US Cities.

Loughnan M, Nicholls N and Tapper NJ (2012) Mapping Heat Health Risks in Urban Areas. International Journal of Population Research 2012.

McClure E, Feinstein L, Cordoba E, et al. (2019) The legacy of redlining in the effect of foreclosures on Detroit residents' self-rated health. Health & place 55: 9–19. [PubMed: 30448354]

Mitchell B and Franco J (2016) HOLC" REDLINING" MAPS: The Persistent Structure of Segregation and Economic Inequality. NCRC.

Namin S, Xu W, Zhou Y, et al. (2020) The legacy of the Home Owners' Loan Corporation and the political ecology of urban trees and air pollution in the United States. Social Science & Medicine 246: 112758. [PubMed: 31884239]

Nardone A, Casey JA, Morello-Frosch R, et al. (2020a) Associations between historical residential redlining and current age-adjusted rates of emergency department visits due to asthma across eight cities in California: an ecological study. The Lancet Planetary Health 4(1): e24–e31. [PubMed: 31999951]

Nardone A, Casey JA, Rudolph KE, et al. (2020b) Associations between historical redlining and birth outcomes from 2006 through 2015 in California. PloS one 15(8): e0237241. [PubMed: 32764800]

Nardone A, Rudolph KE, Morello-Frosch R, et al. (2021) Redlines and Greenspace: The Relationship between Historical Redlining and 2010 Greenspace across the United States. Environmental health perspectives 129(1): 017006.

Nayak S, Shrestha S, Kinney P, et al. (2018) Development of a heat vulnerability index for New York State. Public Health 161: 127–137. [PubMed: 29195682]

Nowak DJ and Greenfield EJ (2018) Declining urban and community tree cover in the United States. Urban forestry & urban greening 32: 32–55.

Petkova EP, Horton RM, Bader DA, et al. (2013) Projected heat-related mortality in the US urban northeast. International Journal of Environmental Research and Public Health 10(12): 6734–6747. [PubMed: 24300074]

Reid CE, O'neill MS, Gronlund CJ, et al. (2009) Mapping community determinants of heat vulnerability. Environmental health perspectives 117(11): 1730–1736. [PubMed: 20049125]

Rosenthal JK, Kinney PL and Metzger KB (2014) Intra-urban vulnerability to heat-related mortality in New York City, 1997–2006. Health & place 30: 45–60. [PubMed: 25199872]

Ross CE and Mirowsky J (2001) Neighborhood disadvantage, disorder, and health. Journal of health and social behavior. 258–276. [PubMed: 11668773]

Rothstein R (2017) The color of law: A forgotten history of how our government segregated America. Liveright Publishing.

Sadler RC and Lafreniere DJ (2017) Racist housing practices as a precursor to uneven neighborhood change in a post-industrial city. Housing studies 32(2): 186–208.

Sailor DJ, Baniassadi A, O'Lenick CR, et al. (2019) The growing threat of heat disasters. Environmental Research Letters 14(5): 054006.

Samuelson H, Baniassadi A, Lin A, et al. (2020) Housing as a critical determinant of heat vulnerability and health. Science of the total environment 720: 137296.

Santamouris M, Paolini R, Haddad S, et al. (2020) Heat mitigation technologies can improve sustainability in cities. An holistic experimental and numerical impact assessment of urban overheating and related heat mitigation strategies on energy consumption, indoor comfort, vulnerability and heat-related mortality and morbidity in cities. Energy and Buildings 217: 110002.

Schaffer A, Muscatello D, Broome R, et al. (2012) Emergency department visits, ambulance calls, and mortality associated with an exceptional heat wave in Sydney, Australia, 2011: a time-series analysis. Environmental Health 11(1): 3. [PubMed: 22273155]

Schell CJ, Dyson K, Fuentes TL, et al. (2020) The ecological and evolutionary consequences of systemic racism in urban environments. Science 369(6510).

Stone B Jr and Rodgers MO (2001) Urban form and thermal efficiency: how the design of cities influences the urban heat island effect. American Planning Association. Journal of the American Planning Association 67(2): 186.

Streutker DR (2003) Satellite-measured growth of the urban heat island of Houston, Texas. Remote Sensing of Environment 85(3): 282–289.

Thacker MT, Lee R, Sabogal RI, et al. (2008) Overview of deaths associated with natural events, United States, 1979–2004. Disasters 32(2): 303–315. [PubMed: 18380857]

Weber S, Sadoff N, Zell E, et al. (2015) Policy-relevant indicators for mapping the vulnerability of urban populations to extreme heat events: A case study of Philadelphia. Applied Geography 63: 231–243.

White H (1980) A heteroskedasticity-consistent covariance matrix estimator and a direct test for heteroskedasticity. Econometrica: journal of the Econometric Society. 817–838.

Wilson B (2020) Urban Heat Management and the Legacy of Redlining. Journal of the American Planning Association. 1–15.

Yin C, Yuan M, Lu Y, et al. (2018) Effects of urban form on the urban heat island effect based on spatial regression model. Science of the total environment 634: 696–704.

Zenou Y and Boccard N (2000) Racial discrimination and redlining in cities. Journal of Urban economics 48(2): 260–285.

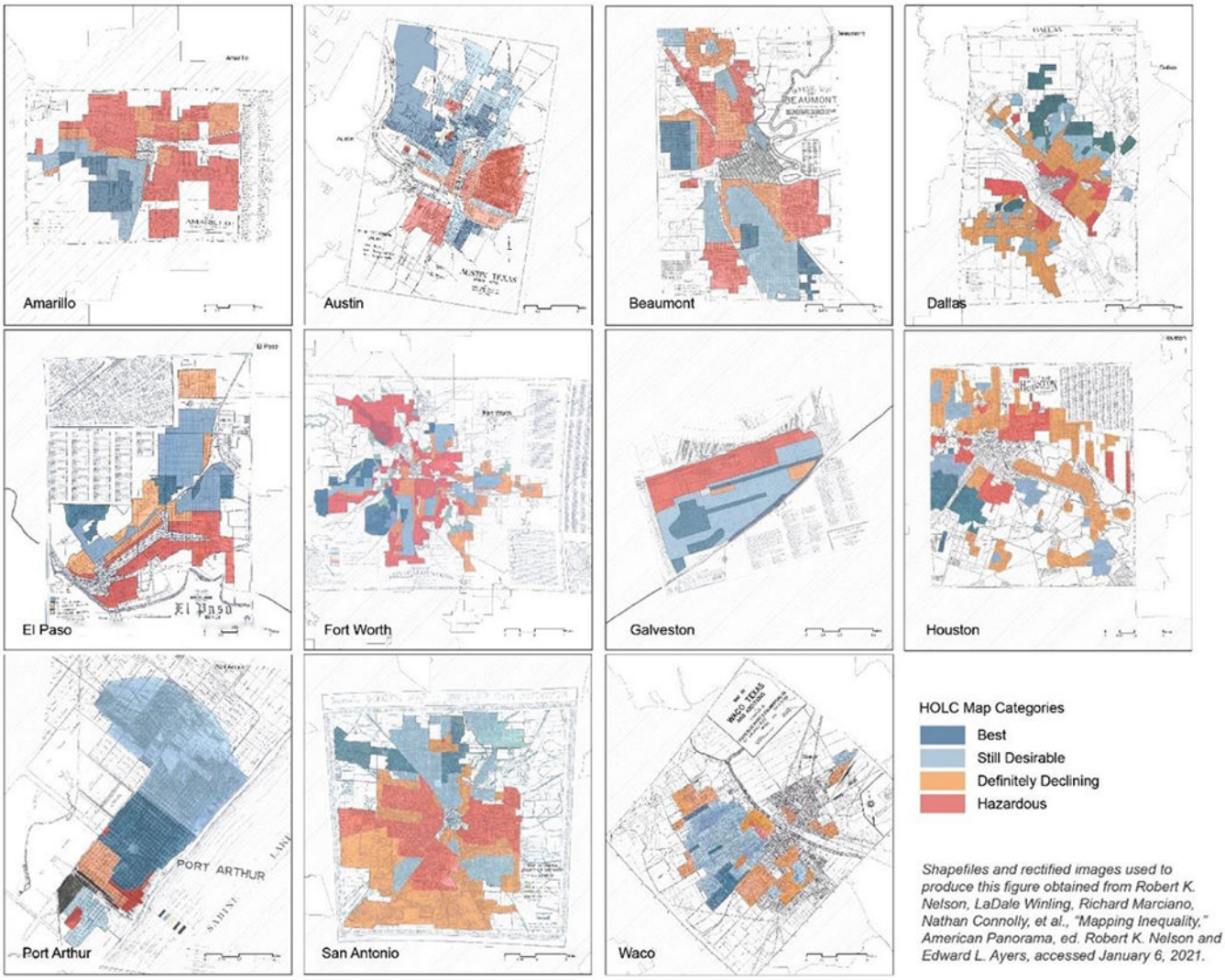

Figure 1.
HOLC redlining maps of selected cities.

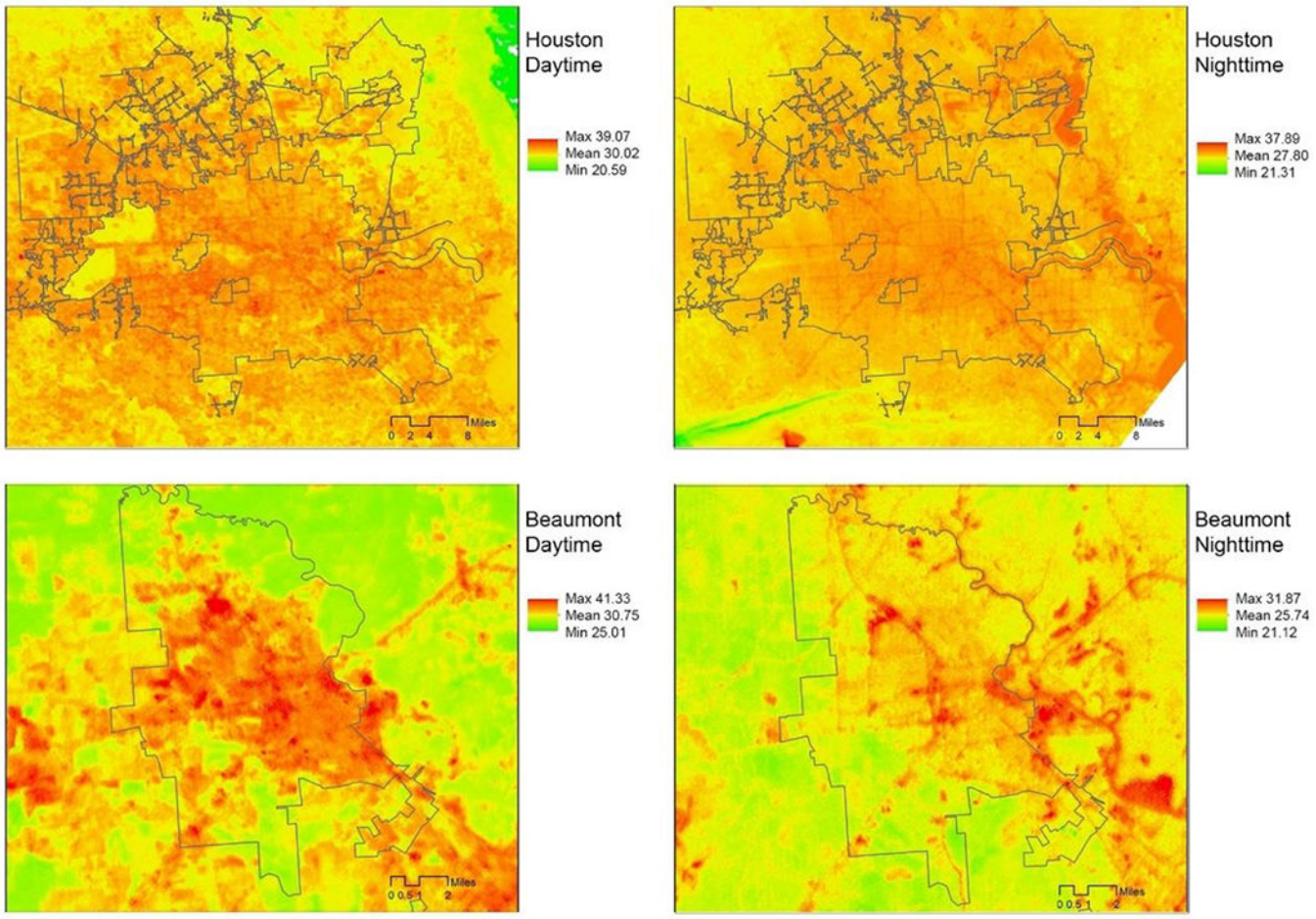

Figure 2.
Example daytime and nighttime LST (Houston and Beaumont)

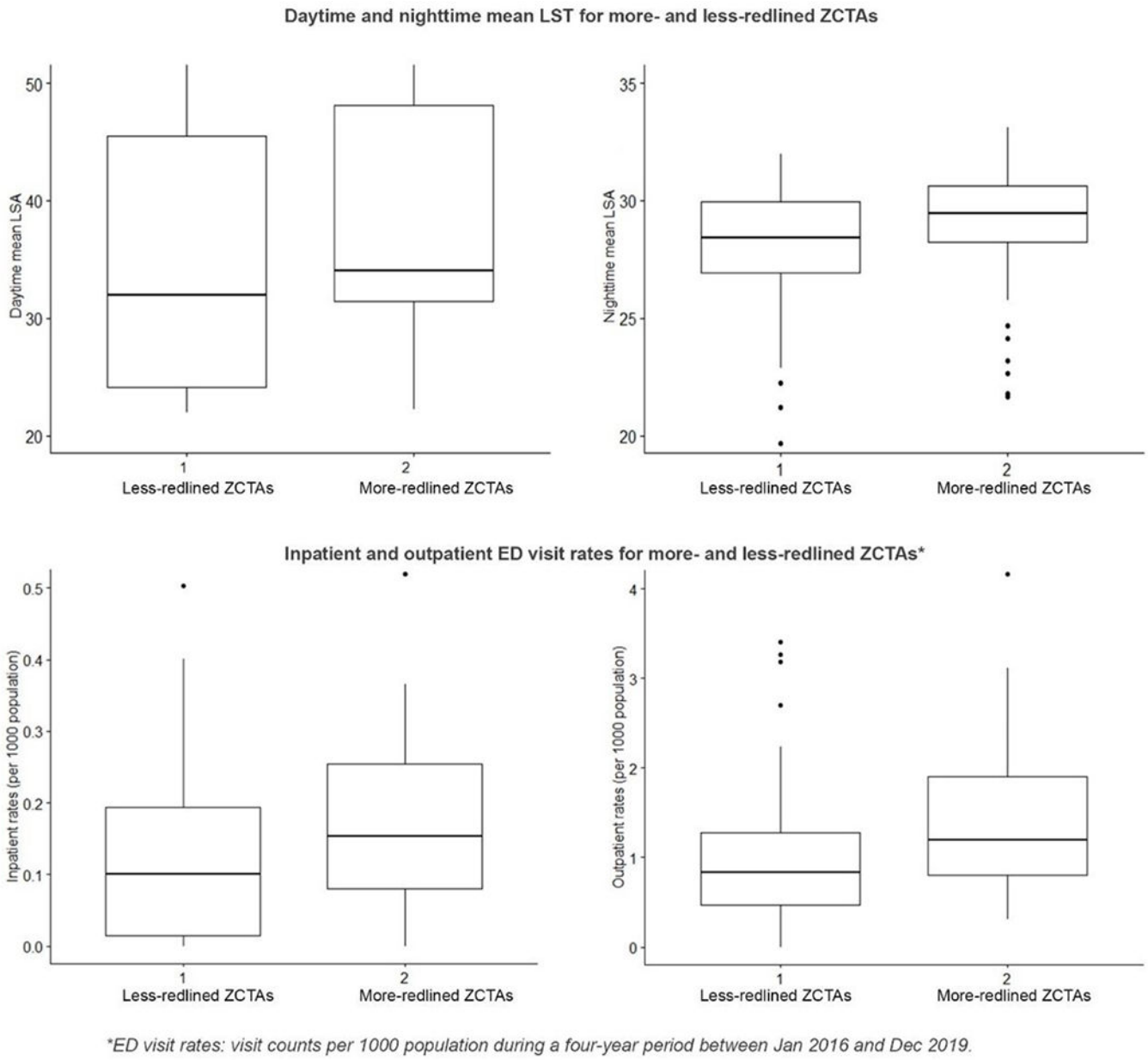

Figure 3.
Comparisons of LST and ED visits between more- and less- redlined neighborhoods

Table 1.

Descriptive statistics of variables and comparisons between more- and less-redlined ZCTAs

Variables	Entire sample		Areas with lower percentage of redlined zones		Areas with higher percentage of redlined zones		Diff[1]
	Mean	SD	Mean	SD	Mean	SD	
Social vulnerability							
Total population (k)	24.3866	14.7761	25.5494	14.5866	23.2079	14.9722	ns.
Housing unit (k)	10.1965	6.0726	10.6301	5.8798	9.7571	6.2713	ns.
Population 65 or older (%)	18.2823	10.3947	17.8785	9.0607	18.6916	11.6406	ns.
Non-White population (%)	29.9844	17.3154	28.5387	17.6139	31.4497	17.0011	ns.
Hispanic population (%)	44.7117	27.6254	35.0949	24.7502	54.4584	27.1100	p<0.001
Low income (%)	21.2043	11.2586	17.5768	12.0116	24.8808	9.1383	p<0.001
Living alone (%)	54.1347	13.3397	49.1364	15.3207	59.2005	8.4349	p<0.001
Speak English not well or not at all (%)	9.4919	8.4780	6.6575	7.3061	12.3647	8.6598	p<0.001
Heat Exposure							
Daytime LST (°C)	36.1718	9.5707	34.2368	9.4586	38.1330	9.3419	p<0.01
Daytime min LST (°C)	29.2809	7.6504	27.1543	7.4309	31.4362	7.3029	p<0.01
Daytime max LST (°C)	42.0879	12.3153	40.5444	12.7614	43.6522	11.7251	ns.
Nighttime LST (°C)	28.5523	2.5390	28.1205	2.4368	28.9899	2.5816	p<0.05
Nighttime min LST (°C)	25.3793	3.2214	24.7777	3.4524	25.9889	2.8651	ns.
Nighttime max LST (°C)	32.1426	2.7758	31.9356	2.8813	32.3524	2.6678	p<0.05
Heat-Related Emergence Department Visit							
Inpatient admission rates (per 1000 population)	0.2179	0.4421	0.1543	0.300	0.2824	0.5446	p<0.01
Outpatient admissions rates (per 1000 population)	1.4775	1.8743	1.1825	1.4176	1.7764	2.2147	p<0.01

[1]Results from independent t-test or Wilcoxon test based on distributions.

ns. Nonsignificant.

Table 2.

Spatial lag models of daytime and nighttime LST with redlining.

	Model 1 - Daytime LST				Model 2 - Nighttime LST			
Variables			95% CI				95% CI	
	Estimate	**SE**	**Low**	**High**	**Estimate**	**SE**	**Low**	**High**
rho	0.9552	0.0098	0.9360	0.9744	0.8937	0.0218	0.8510	0.9364
(Intercept)	1.3660***	0.3770	0.6271	2.1048	2.8047***	0.6182	1.5930	4.0163
Redlining								
Area redlined as definitely declining or hazardous (%)	0.0122**	0.0042	0.0039	0.0205	0.0098***	0.0025	0.0050	0.0146

** $p < 0.01$,

*** $p < 0.001$

Table 3.

Regression models of inpatient rates with social vulnerability and redlining.

Variables	Inpatient Admission Rates with Heat-Related Diagnosis[1]							
	Model 3 - Social				Model 4 − Social + Redlining			
			95% CI				95% CI	
	Estimate	SE	Low	High	Estimate	SE	Low	High
(Intercept)	−0.1739 $^{+}$	0.0883	−0.3484	0.0006	−0.1426	0.0886	−0.3177	0.0325
Social Vulnerability								
Population 65 or older (%)	0.0076 ***	0.0021	0.0034	0.0118	0.0084 ***	0.0021	0.0042	0.0126
Non-White population (%)	−0.0016	0.0015	−0.0045	0.0013	−0.0011	0.0015	−0.0040	0.0019
Hispanic population (%)	−0.0007	0.0012	−0.0030	0.0016	−0.0009	0.0012	−0.0032	0.0014
Low income (%)	0.0089 ***	0.0026	0.0038	0.0139	0.0082 **	0.0025	0.0031	0.0132
Living alone (%)	0.0055 **	0.0020	0.0016	0.0095	0.0042 *	0.0021	0.0002	0.0083
Speak English not well or not at all (%)	−0.0006	0.0037	−0.0078	0.0067	−0.0011	0.0036	−0.0082	0.0061
Redlining								
Area redlined as definitely declining or hazardous (%)					0.0018 *	0.0009	0.0001	0.0035

$^{+}$ $p < 0.1$,

* $p < 0.05$,

** $p < 0.01$,

*** $p < 0.001$

[1]. Inpatient admission rates were square root transformed.

Table 4.

Spatial error models of outpatient rates with social vulnerability and redlining.

Variables	Outpatient Visit Rates with Heat-Related Diagnosis[1]							
	Model 5 - Social				Model 6 − Social + Redlining			
			95% CI				95% CI	
	Estimate	SE	Low	High	Estimate	SE	Low	High
(Intercept)	0.0984	0.1747	−0.2441	0.4408	0.1483	0.1733	−0.1915	0.4880
Social Vulnerability								
Population 65 or older (%)	0.0077*	0.0036	0.0005	0.0148	0.0082*	0.0036	0.0012	0.0152
Non-White population (%)	−0.0009	0.0029	−0.0065	0.0047	−0.0005	0.0028	−0.0060	0.0050
Hispanic population (%)	−0.0023	0.0026	−0.0075	0.0028	−0.0025	0.0026	−0.0076	0.0025
Low income (%)	0.0197***	0.0042	0.0114	0.0279	0.0185***	0.0042	0.0103	0.0266
Living alone (%)	0.0110**	0.0035	0.0041	0.0179	0.0096**	0.0035	0.0028	0.0165
Speak English not well or not at all (%)	−0.0030	0.0075	−0.0176	0.0116	−0.0055	0.0074	−0.0200	0.0090
Redlining								
Redlined as definitely declining or hazardous (%)					0.0036*	0.0015	0.0007	0.0066
lambda	0.4769	0.0815	0.3172	0.6365	0.4892	0.0802	0.3320	0.6464

*
p < 0.05,

**
p < 0.01,

***
p < 0.001

1
. Outpatient admission rates were square root transformed.